Available at
www.ElsevierComputerScience.com
POWERED BY SCIENCE DIRECT

Signal Processing 86 (2006) 2185–2197

SIGNAL PROCESSING

www.elsevier.com/locate/sigpro

A novel approach for estimating multi-user interference in impulse radio UWB networks: The pulse collision model

Guerino Giancola, Maria-Gabriella Di Benedetto*

INFOCOM Department, University of Rome La Sapienza, Via Eudossiana, 18-00184, Rome, Italy

Received 1 March 2005; accepted 31 October 2005
Available online 13 February 2006

Abstract

Modeling Multi-User Interference (MUI) is crucial in the design of wireless networks. In the case of Impulse Radio (IR)-Ultra Wide Band (UWB) networks, most of the adopted models are inspired by the legacy of the reference literature on spread spectrum communications, and do not address specific features for IR systems, where spectrum spreading is basically obtained by the radiation of very short time-limited pulses. The problem of conceiving a specific model for MUI in IR-UWB networks is addressed in this paper. The reference scenario consists of multiple asynchronous users transmitting IR-UWB signals using Pulse Position Modulation (PPM) in combination with Time Hopping (TH) coding. We provide a novel analytical expression for the average BER based on the observation that interference in IR is provoked by collisions occurring between pulses belonging to different transmissions. The proposed method requires specification of a similar set of system parameters as Gaussian-based approaches, but shows improved accuracy in estimating BER.

Keywords: Ultra Wide Band; Multi-user interference; Impulse Radio; Pulse collision

1. Introduction

Different methods have been proposed in the recent past for evaluating the effect of Multi-user Interference (MUI) on the performance of Impulse Radio-Ultra Wide Band (IR-UWB) networks [1]. Most of the above methods are inspired by the legacy of the reference literature on Spread Spectrum (SS) communications, in which significant emphasis is given to the analysis of the Code Division Multiple Access (CDMA) case, with particular focus on 3G CDMA networks.

First models for MUI in CDMA networks were based on the standard Gaussian approximation (SGA). The SGA relies on the observation that when MUI is provoked by the sum of a large number of users, interference can be treated as an additive Gaussian noise with uniform power spectrum over the frequency band of interest. Under this assumption, receiver tolerance to MUI easily expresses as a function of the average signal to noise ratio at the reference receiver, where noise power is calculated as the sum of thermal noise and average MUI powers. The use of the SGA for modelling MUI was first introduced by Pursley [2] in an attempt to assess the multiple access capabilities of a Direct Sequence (DS) CDMA system operating over an ideal AWGN channel and

*Corresponding author. Tel.: +39 06 487 33 00.
E-mail address: dibenedetto@newyork.ing.uniroma1.it (M.-G. Di Benedetto).

0165-1684/$ - see front matter © 2006 Elsevier B.V. All rights reserved.
doi:10.1016/j.sigpro.2005.10.023

employing ideal rectangular (band-unlimited) chip waveforms. The work in [2] was further extended in order to encompass the adoption of band-limited chip waveforms [3] and propagation over multipath-affected channels [4]. The unchallenged success of the SGA resides in two basic features: (i) it is *simple*, i.e., few system parameters are required for evaluating performance; (ii) it is *fast*, i.e., the average BER is provided through an explicit form which can be calculated at a reduced computational cost. Such properties have also proved to be very effective for deriving admission control policies and power allocation strategies for multi-user CDMA-based networks [5–9]. The SGA, however, is based on the central limit theorem, and provides thus accurate BER estimations only for scenarios with high MUI levels, i.e., for densely populated networks [10]. Specifically, the SGA was shown to provide accurate BER estimations when MUI yields to a measured BER higher than 10^{-3}. Contrarily, the gap between theoretical and measured BERs may be as large as several orders of magnitude when scenarios with low MUI are taken into account [11].

In order to comply with the SGA inaccuracy in scarcely populated networks, modifications of the original method have been suggested, such as the Improved Gaussian Approximation (IGA) proposed by Morrow and Lehnert [12] and Morrow and Lehnert [13]. By the IGA, system performance is determined by first computing the conditional BER for a generic value of the MUI power, and by then averaging over all possible MUI power values. Contrarily to the SGA, which evaluates BER at *average operating conditions*, the IGA *averages the BER* over all possible MUI scenarios. IGA proved to be more accurate than SGA, also for scarcely populated networks or systems with dominating interferers [10]. In particular, BER estimation by the IGA was shown to match BER curves obtained by simulation for values as low as 10^{-6} [14]. The IGA, however, is neither *simple* nor *fast* to implement. This method, in fact, requires the evaluation of the probability density function of the MUI power, which is not an easy task for several operating conditions. In [12], for example, results are only provided for the simple scenario where all interfering signals are received with same power of the useful signal, and thermal noise is not present at the reference receiver. Based on the IGA approach, a Simplified IGA (SIGA) method was first proposed by Holtzman [15], and then extended by Morrow [16] and Nguyen and Shwedyk [17]. With the SIGA method, the knowledge of the probability density function of the MUI power is not required, since the BER is computed by means of approximations. In particular, the BER is expressed as an expansion in differences, with parameters derived as in [18]. SIGA BER expressions present an accuracy which is comparable to that of IGA, but with a computational complexity which is comparable to that of SGA. BER estimations by SIGA, however, closely fit simulation data only when power control is implemented at the reference receiver. In this case, the accuracy of SIGA is verified for BER values as low as 10^{-5} [15]. When the hypothesis of power control is removed, SIGA dramatically decreases in accuracy, in particular when systems with dominating interferers are taken into account [10,14,19].

An alternative to the above Gaussian-based approaches is given by the Characteristic Function (CF) method, which was initially proposed by Geraniotis and Pursley [20] for DS-CDMA systems with interfering users received with equal power and deterministic codes. This work was then extended by Geraniotis and Ghaffari [21] to the case of non-deterministic codes, and by Corazza et al. [22] in order to remove the hypothesis of power control at the reference receiver. The CF method is not original, since it was formerly introduced for determining the average symbol error rate in single-user communications affected by inter-symbol interference [23,24]. When applied to MUI estimation, the CF method provides exact analytical expressions for the average BER. These expressions, however, include both open-ended and finite integrals, which can be computed only by numerical evaluation through the Simpson's rule, for example, or by the trapezoid approximation [25]. Depending on the computational complexity that can be afforded for solving such integrals, the estimate is more or less accurate. Computational complexity can be reduced in special operating conditions, as for example, when PSK modulation techniques are taken into account [20], but it remains the major drawback of the CF method.

A non-Gaussian approach to MUI estimation for SS systems was also proposed by Laforgia et al. [26]. Similarly to the CF method, the average probability of error is expressed by means of integration formulas. In this case, however, the Gaussian Quadrature Rule (GQR) is used for simplifying the numerical evaluation of such integrals [27]. The use of the GQR method in communication systems was initially introduced for evaluating performance in optical fiber transmission systems [28] and in wireless channels affected by inter-symbol interference [29]. When applied to the case of multi-user CDMA systems, the GQR technique guarantees an accuracy in estimating BER which is comparable to that achievable with the CF method, but with reduced computational complexity. The problem with GQR is that it requires a high number of moments (from 10 to 20) for characterizing the MUI random process. If such information is not available, as it usually happens in practical situations, numerical routines are necessary for evaluating the moments, with consequently an increase of computational time. In [26], the GQR technique is applied to the special case of DS-CDMA signals propagating over an AWGN channel, but the analysis was then extended in [30,31] to the case of multipath-affected channels.

At first glance, IR-UWB technology is based on the same principles of conventional SS-CDMA, i.e., spectral expansion of the waveform generated by the user, and adoption of different codes for allowing different users to share the same radio resource. As a consequence, each of the above MUI models can be theoretically extended to the case of IR-UWB systems. Earlier contributions to interference estimation in IR-UWB networks were based in fact on the SGA approach [32,33]. Under the SGA, receiver tolerance to MUI simply depends upon the processing gain of the system, which is defined as the ratio between the total bandwidth used for transmission and the bit rate of the reference user. The higher the processing gain, the higher the number of devices which can simultaneously access the physical medium for a target performance. Simplicity of BER estimation under the SGA favored the development of several resource allocation algorithms for both centralized and distributed IR-UWB networks [34–37]. Further investigations showed, however, as in the CDMA case, that the SGA provides weak estimations of the average BER when low values of user bit rate [38] or sparse topologies [39] are considered. An asymptotic study on the validity of the Gaussian approximation for IR-UWB was also proposed by Fiorina and Hachem [40], based on the Lindeberg's condition [41]. Results of Fiorina and Hachem [40] show that for both Pulse Position Modulation (PPM) and Pulse Amplitude Modulation (PAM) signal formats the probability distribution of MUI is Gaussian provided that both the number of pulses per bit and system processing gain tend to infinity.

Recent papers [42–44] apply the CF approach for deriving highly accurate BER expressions, but at the price of an increased computational complexity. In [42], Hu and Beaulieu derive exact average BER expressions for IR-UWB systems based on PPM and PAM in combination with Time Hopping (TH) coding, in the case of propagation over an AWGN channel. BER estimation requires the numerical evaluation of open-ended integrals, but guarantees an excellent fit of theoretical vs. simulated data for BER values as low as 10^{-10}. In [43], Forouzan et al. apply the CF method for estimating the performance of PPM–TH systems in a scenario where all users are received with equal power, and the presence of thermal noise at the reference receiver is neglected. In such a scenario, a BER expression with reduced complexity is derived by introducing a linear approximation for the probability density function of the MUI term. In [44], Sabattini et al. evaluate an approximation of the CF function for an ideal PPM–TH system where rectangular pulse waveforms are assumed to propagate over AWGN channels. Under such hypotheses, a closed-form expression for the BER is provided, which was demonstrated to provide accurate BER estimations even in the presence of few interfering users.

In [45], Durisi and Benedetto apply the GQR method to the case of IR-UWB signals propagating over AWGN channels, and provide a BER expression which was demonstrated to very well fit simulation data when 13 moments of the MUI term are introduced within the computation.

Innovative approaches to MUI modeling for IR-UWB were proposed by Fontana [46] and by Di Benedetto et al. [47]. In [46], interference provoked by IR-UWB signals at the output of a band-pass filter is modeled as a filtered Poisson random signal characterized by an average count rate λ (pulse inter-arrival time). It is shown that when λ is large, the interference provoked by an UWB signal tends to a Gaussian random process. In [47], MUI is analyzed under a novel perspective that explicitly takes into account the peculiar way in which information is structured in IR transmissions, that is, MUI is modeled based on the observation that interference in IR is provoked by collisions occurring between pulses belonging to different transmissions. Average probability of error is expressed in [47] as the product of two contributions: (i) the average probability of having at least one collision at the input of the reference receiver; (ii) the average probability of error on the bit, conditioned on the event that one or more collisions have occurred at the receiver input. For both the above terms, an analytical expression is provided under rather simplistic hypotheses, i.e., without introducing a receiver structure.

The present work extends [47] by redefining both the events of pulse collision and bit error based on a complete receiver structure definition. In particular, the model for the receiver includes soft detection which produces an estimate of a current bit value by collecting information conveyed by the set of pulses representing it. In addition, we introduce a refined definition for the probability of bit error given that one or more collisions have occurred, which also incorporates the effect of thermal noise in the receiver. A novel analytical expression for the average BER is then provided for the case of IR-UWB signals employing PPM in combination with TH coding, and propagating over AWGN channels. Power control at the reference receiver is not required for BER computation under the proposed approach.

This paper is organized as follows. Section 2 defines the system model. Section 3 describes the novel method for MUI estimation, and compares the proposed MUI model with already available models in terms of computational complexity and required knowledge of systems parameters. Section 4 validates the proposed MUI model by simulation of different network scenarios. Finally, Section 5 concludes the paper.

2. System model

The system model analyzed in this paper consists of a reference transmitter TX which emits IR-UWB-TH-PPM signals to a reference receiver RX. The binary sequence **b** generated by TX is formed by independent and identically distributed random variables with equally probable symbols "0" and "1". The transmitted signal writes:

$$s_{\mathrm{TX}}(t) = \sqrt{E_{\mathrm{TX}}}\sum_j p_0\Big(t - jT_{\mathrm{S}} - \theta_j - \varepsilon b_{\lfloor j/N_{\mathrm{S}}\rfloor}\Big), \tag{1}$$

where $p_0(t)$ is the energy-normalized waveform of the transmitted pulses, E_{TX} is the energy of each pulse, T_{S} is the average pulse repetition period, $0 \leqslant \theta_j < T_{\mathrm{S}}$ is the time shift of the jth pulse provoked by the TH code, ε is the PPM shift, b_x is the xth bit of **b**, N_{S} is the number of pulses transmitted for each bit, and $\lfloor x \rfloor$ is the inferior integer part of x. According to (1), the PPM modulator introduces a delay ε on all N_{S} pulses corresponding to a "1" bit.

A general flat AWGN channel model is assumed. The impulse response for the channel between TX and RX is given by $h(t) = \alpha\delta(t-\tau)$, where α and τ are the amplitude gain and propagation delay. TX and RX are assumed to be perfectly synchronized, i.e., RX has perfect knowledge of τ. The channel output is corrupted by thermal noise and MUI generated by N_i interfering IR-UWB devices. The received signal thus writes:

$$s_{\mathrm{RX}}(t) = r_{\mathrm{u}}(t) + r_{\mathrm{mui}}(t) + n(t), \tag{2}$$

where $r_{\mathrm{u}}(t)$, $r_{\mathrm{mui}}(t)$, and $n(t)$ are the useful signal, MUI, and thermal noise, respectively. As regards $r_{\mathrm{u}}(t)$, one has:

$$r_{\mathrm{u}}(t) = \sqrt{E_{\mathrm{u}}}\sum_j p_{\mathrm{o}}\Big(t - jT_{\mathrm{S}} - \theta_j - \varepsilon b_{\lfloor j/N_{\mathrm{S}}\rfloor} - \tau\Big), \tag{3}$$

where $E_{\mathrm{u}} = \alpha^2 E_{\mathrm{TX}}$.

As regards $r_{\mathrm{mui}}(t)$, we assume that all interfering signals are characterized by same T_{S}, and thus:

$$r_{\mathrm{mui}}(t) = \sum_{n=1}^{N_i}\sqrt{E^{(n)}} \times \sum_j p_{\mathrm{o}}\left(t - jT_{\mathrm{S}} - \theta_j^{(n)} - \varepsilon b^{(n)}_{\lfloor j/N_{\mathrm{S}}^{(n)}\rfloor} - \tau^{(n)}\right), \tag{4}$$

where $E^{(n)}$ and $\tau^{(n)}$ are received energy per pulse and delay for the nth interfering user. The relative delay $\Delta\tau^{(n)} = \tau - \tau^{(n)}$ is assumed to be a random variable uniformly distributed between 0 and T_{S}. The terms $\theta_j^{(n)}$, $b_x^{(n)}$ and $N_S^{(n)}$ in (4) are the time shift of the jth pulse, the xth bit generated by user n, and the number of pulses per bit for the nth transmitter, respectively. In the present system model, both TH codes and data bit sequences are randomly generated and correspond to pseudo-noise sequences, that is, $\theta_j^{(n)}$ terms are assumed to be independent random variables uniformly distributed in the range $[0,T_{\mathrm{S}})$, and $b_x^{(n)}$ values are assumed to be independent random variables with equal probability to be "0" or "1".

Finally, signal $n(t)$ in (2) is Gaussian noise, with double-sided power spectral density $N_0/2$.

The optimum single-user receiver for the above system model is composed by a coherent correlator followed by a ML detector [1]. In every bit period $T_{\mathrm{b}} = N_{\mathrm{S}}T_{\mathrm{S}}$, the correlator converts the received signal of (2) into a decision variable Z, which forms the input of the detector. Soft decision detection is performed, i.e., the signal formed by N_S pulses is considered as a single multi-pulse signal. The received signal is thus cross-correlated with a correlation mask $m(t)$ that is matched with the train of pulses representing one bit. The input of the detector $Z(x)$, for a generic bit b_x, can be thus expressed as follows:

$$Z(x) = \int_{xN_S T_S+\tau}^{(x+1)N_S T_S+\tau} s_{RX}(t) m_x(t-\tau)\,dt = Z_u + Z_{mui} + Z_n, \tag{5}$$

where $m_x(t)$ is the correlation mask for b_x, i.e.

$$m_x(t) = \sum_{j=xN_S}^{(x+1)N_S} (p_0(t - jT_S - \theta_j) - p_0(t - jT_S - \theta_j - \varepsilon)). \tag{6}$$

Eq. (5) indicates that the decision variable $Z(x)$ consists of three terms: the signal term Z_u, the MUI contribution Z_{mui}, and the noise contribution Z_n, which is Gaussian with zero mean and variance $\sigma_n^2 = N_S N_0 \gamma(\varepsilon)$, where $\gamma(\varepsilon) = 1 - R_0(\varepsilon)$, and where $R_0(\varepsilon)$ is defined as the autocorrelation function of the pulse waveform $p_0(t)$:

$$R_0(t) = \int_{-\infty}^{+\infty} p_0(\xi) p_0(\xi - t)\,d\xi. \tag{7}$$

Bit b_x is estimated by comparing the $Z(x)$ term in (5) with a zero-valued threshold according to the following rule: when $Z(x) > 0$ decision is "0", when $Z(x) < 0$ decision is "1". For independent and equiprobable transmitted bits, the average BER at the output of the detector is thus:

$$\begin{aligned}\text{BER} &= \frac{1}{2}\text{Prob}(Z(x) < 0 | b_x = 0) \\ &\quad + \frac{1}{2}\text{Prob}(Z(x) > 0 | b_x = 1) \\ &= \text{Prob}(Z(x) < 0 | b_x = 0).\end{aligned} \tag{8}$$

3. The Pulse Collision model

Under the SGA hypothesis, random variables Z_{mui} and Z_n in (5) would be both modeled as Gaussian random variables with zero mean and variance σ_{mui}^2 and σ_n^2, respectively. With respect to σ_{mui}^2 that can be interpreted as the MUI power at the correlator output at the average operating conditions, one has [1]

$$\sigma_{mui}^2 = \frac{N_S}{T_S} \sigma_M^2 \sum_{n=1}^{N_i} E^{(n)}, \tag{9}$$

where the σ_M^2 term depends upon pulse waveform $p_0(t)$ and value of the PPM shift ε, according to the following relation:

$$\sigma_M^2 = \int_{-\infty}^{+\infty} \left(\int_{-\infty}^{+\infty} p_0(t-\tau)(p_0(t) - p_0(t-\varepsilon))\,dt \right)^2 d\tau. \tag{10}$$

Under the SGA, the average BER writes

$$\text{BER} = \frac{1}{2} \operatorname{erfc}\left(\sqrt{ \frac{1}{2} \left(\left(\frac{N_S E_u \gamma(\varepsilon)}{N_0} \right)^{-1} + \left(\frac{N_S T_S \gamma(\varepsilon)}{\sigma_M^2 \sum_{n=1}^{N_i} (E^{(n)}/E_u)} \right)^{-1} \right)^{-1} } \right). \tag{11}$$

The SGA is derived from the central limit theorem and is thus valid only asymptotically.

We now introduce the proposed model that moves away from the Gaussian approach. Observe that the signal term Z_u in (5) is given by

$$Z_u = \begin{cases} +N_S \sqrt{E_u} \gamma(\varepsilon) & \text{if } b_x = 0, \\ -N_S \sqrt{E_u} \gamma(\varepsilon) & \text{if } b_x = 1, \end{cases} \tag{12}$$

according to which the BER expression in (8) rewrites:

$$\begin{aligned}\text{BER} &= \text{Prob}(N_S \sqrt{E_u} \gamma(\varepsilon) + Z_{mui} + Z_n < 0) \\ &= \text{Prob}(Z_{mui} < -(N_S \sqrt{E_u} \gamma(\varepsilon) + Z_n)) \\ &= \text{Prob}(Z_{mui} < -y),\end{aligned} \tag{13}$$

where y is a Gaussian random variable with mean $N_S \sqrt{E_u} \gamma(\varepsilon)$ and variance $N_S N_0 \gamma(\varepsilon)$.

BER expression in (13) can be evaluated by first computing the conditional BER for a generic y value, and by then averaging over all possible y values, i.e.,

$$\text{BER} = \int_{-\infty}^{+\infty} \text{Prob}(Z_{mui} < -y | y) p_Y(y)\,dy, \tag{14}$$

where $p_Y(y)$ is the Gaussian probability density function of y.

In our approach, conditional probability of error Prob $(Z_{mui} < -y|y)$ takes into account collisions between pulses of different transmissions. In every bit period T_b, the number of possible collisions at the input of the receiver, denoted with N_C, is confined between 0 and $N_S N_i$, given N_S pulses per bit and N_i interfering users. Under the reasonable assumption that the events of collision are independent of one another, the conditional probability of error can be rewritten as follows:

$$\mathrm{Prob}(Z_{\mathrm{mui}} < -y|y) = \sum_{N_C=0}^{N_S N_i} \mathrm{Prob}(Z_{\mathrm{mui}} < -y|y, N_C) P_{CP}(N_C), \tag{15}$$

where $P_{CP}(N_C)$ indicates the probability of having N_C pulse collisions within one single bit interval. When substituting (15) into (14), one obtains

$$\mathrm{BER} = \sum_{N_C=0}^{N_S N_i} P_{CP}(N_C) \times \int_{-\infty}^{+\infty} \mathrm{Prob}(Z_{\mathrm{mui}} < -y|y, N_C) p_Y(y)\, \mathrm{d}y. \tag{16}$$

For independent interferers, $P_{CP}(N_C)$ can be reasonably expressed through the binomial distribution, i.e.,

$$P_{CP}(N_C) = \binom{N_S N_i}{N_C} P_{C0}^{N_C} (1 - P_{C0})^{N_S N_i - N_C}, \tag{17}$$

where P_{C0} is the probability that a single interfering device produces a colliding pulse within T_S. P_{C0} can be computed as the fraction of T_S during which the receiver may be affected by the presence of an interfering pulse and produce non-zero contributions to Z_{mui}, and can thus be expressed as follows:

$$P_{C0} = \frac{\min(2T_M + \varepsilon, 4T_M, T_S)}{T_S}, \tag{18}$$

where T_M is the length of the pulse waveform $p_0(t)$, defined as the period of time in which a given percentage of the pulse energy is contained. Eq. (18) indicates that the time of possible collision is equal to the correlator window $(2T_M + \varepsilon)$, except when $(2T_M + \varepsilon)$ is either four times greater than T_M or greater than T_S.

The next step for estimating BER is to define the shape of the conditional probability of error. We propose here for $\mathrm{Prob}(Z_{\mathrm{mui}} < -y|y, N_C)$ the linear model shown in Fig. 1 and analytically expressed by:

$$\mathrm{Prob}(Z_{\mathrm{mui}} < -y|y, N_C) = \begin{cases} 1 & \text{for } y \leqslant -Z_{\max}(N_C), \\ 1 - \frac{P_{CP}(N_C)}{2}\left(1 + \frac{y}{Z_{\max}(N_C)}\right) & \text{for } -Z_{\max}(N_C) < y \leqslant 0, \\ \frac{P_{CP}(N_C)}{2}\left(1 - \frac{y}{Z_{\max}(N_C)}\right) & \text{for } 0 < y \leqslant Z_{\max}(N_C), \\ 0 & \text{for } y > Z_{\max}(N_C), \end{cases} \tag{19}$$

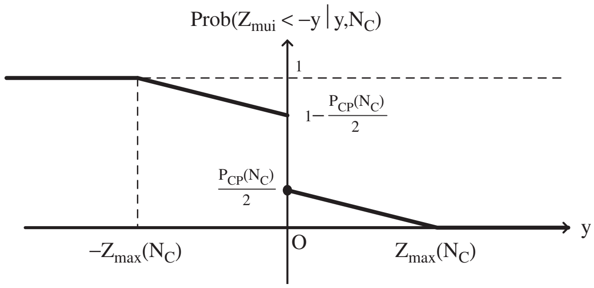

Fig. 1. Linear model for the conditional probability of error $\mathrm{Prob}(Z_{\mathrm{mui}} < -y|y, N_C)$, given y and given N_C.

where $Z_{\max}(N_C)$ is defined as the maximum value for the MUI term Z_{mui}, when N_C collisions have occurred at the reference receiver.

The selection of a linear model for the conditional probability of error simplifies the analytical derivation of the BER at the reference receiver. Moreover, it was shown in [43] that the cumulative density function of MUI caused by one single interferer can be reasonably fitted by a linear function. Based on [43], we propose the linear model in (19), which includes multiple interferers with different received powers. The model in (19) was selected on the basis of both practical observations and statistical results emerged by simulation. First, the model in (19) reflects the observation that for a given number of collision N_C, an error occurs with probability 1 if the sum of Z_u and Z_n, i.e. y, is negative and lower than $-Z_{\max}(N_C)$. Such a probability of error decreases with y, and becomes 0 when y is positive and higher than $Z_{\max}(N_C)$. In this case, in fact, MUI does not provoke an error since the interference contribution at the receiver output is below y. Secondly, the expression in (19) foresees the presence of a discontinuity in $y = 0$ for the conditional probability of error $\mathrm{Prob}(Z_{\mathrm{mui}} < -y|y, N_C)$. Such a discontinuity was introduced in our model for approximating the peak in $y = 0$ that emerges in the probability density function of the MUI term for PPM receiver structures. As indicated in Eq. (6), in fact, the decision variable for a PPM system is given by the subtraction of two separate contributions. As a consequence, interfering pulses at the receiver input may produce "zero" contributions at the receiver output even when their positions in time fall within the correlator window. This happens, for example, when the relative delay of a single interfering pulse with respect to the reference pulse is half the value of the PPM shift.

According to (19), knowing $Z_{\max}(N_C)$ is required for computing $\mathrm{Prob}(Z_{\mathrm{mui}} < -y|y, N_C)$. In the special case of power control at RX, that is all interfering as well as reference signals have same power at RX, $Z_{\max}(N_C)$ easily expresses as follows:

$$Z_{\max}(N_C) = N_C\sqrt{E_u}. \tag{20}$$

When power control is not implemented at RX, the maximum value of MUI depends on the interfering pattern at the receiver. Specifically, for a given N_C, there are as many $Z_{\max}(N_C)$ possible values as the number of possible combinations of N_C collisions among the N_i interfering users. For a given N_C, however, different estimates for $Z_{\max}(N_C)$ can be obtained as will be discussed below.

A first estimate for $Z_{\max}(N_C)$ can be obtained under the assumption of a "worst case" scenario where interference is always provoked by those users with the highest interfering energies. In this case, one has:

$$Z_{\max}^{(\mathrm{worst})}(N_C) = \sum_{j=1}^{N_i} M(j, N_C)\sqrt{E_S^{(j)}}, \tag{21}$$

where

$$M(j, N_C) = \max\{0, \min\{N_S, N_C - N_S(j-1)\}\} \tag{22}$$

and where $E_S^{(1)}, E_S^{(2)}, \ldots, E_S^{(N_i)}$ are the interfering energies $E^{(1)}, E^{(2)}, \ldots, E^{(N_i)}$ of (4), sorted in descending order that is $E_S^{(j)}, E_S^{(j+1)}$, for $j \in [1, \mathrm{Ni}-1]$. For a given set of interfering energies, $Z_{\max}$ can be computed based on (21), and only depends upon N_C. Computer simulation of different node topologies and corresponding different sets of interfering energies showed that the "worst case" assumption ceases to be valid and leads to unrealistic over-estimates of MUI, when interfering energies are extremely different from one another such as in the case of a few dominating interferers.

An opposite approach consists in assuming a "best case" scenario where collisions are provoked by those users with lowest interfering energies. In this case, one has:

$$Z_{\max}^{(\mathrm{best})}(N_C) = \sum_{j=1}^{N_i} \mu(j, N_C)\sqrt{E_S^{(j)}}, \tag{23}$$

where:

$$\mu(j, N_C) = \max\{0, \min\{N_S, N_C - N_S(N_i - j)\}\}. \tag{24}$$

As for the worst case, computer simulations were performed. Results showed that the $Z_{\max}(N_C)$ estimate obtained by application of (23) strongly under-estimates MUI, when interferers are characterized by largely different power levels.

A third possible approach models interference by assuming interfering pulses with same amplitude A_m. Amplitude A_m is obtained by averaging over all effectively received amplitude values and is thus expressed by:

$$A_m = \frac{1}{N_i}\sum_{j=1}^{N_i}\sqrt{E^{(i)}}. \tag{25}$$

Eq. (25) models an "average" interfering pattern, and we thus define this case as the "average case" scenario. At the correlator output, the interference term is:

$$Z_{\max}^{(\mathrm{average})}(N_C) = N_C A_m. \tag{26}$$

As expected, when severe near–far effects are present, the "average amplitude" hypothesis weakly reflects the interfering pattern at RX and therefore (26) fails in estimating MUI.

In order to improve the accuracy of MUI estimates in those cases where the above models fail, that is, for near–far affected systems, we consider an "intermediate case" where $Z_{\max}(N_C)$ is computed similarly to (21), that is by privileging dominating interferers, but taking into account the presence of interferers with lower powers. The proposed estimate for $Z_{\max}(N_C)$ is in this case expressed as follows:

$$Z_{\max}^{(\mathrm{int})}(N_C) = \sum_{j=1}^{N_i}\left(\left\lceil\frac{N_C - j + 1}{N_i}\right\rceil\sqrt{E_S^{(j)}}\right). \tag{27}$$

Fig. 2 shows the $Z_{\max}(N_C)$ values obtained under the four different assumptions corresponding to: (i) "worst case" (upward triangles on figure, see (21)); (ii) "best case" (downward triangles on figure, see (23)); (iii) "average case" (squares on figure, see (26)); and (iv) "intermediate case" (crosses on figure, see (27)), as a function of number of collisions N_C. These values were computed for a specific set of parameters defined as follows: $N_i = 5$, $N_S = 2$, and interfering energies (assumed to be in (volts)^2) $E^{(1)} = 1/8\,\mathrm{V}^2$, $E^{(2)} = 1/2\,\mathrm{V}^2$, $E^{(3)} = 1\,\mathrm{V}^2$, $E^{(4)} = 2\,\mathrm{V}^2$, $E^{(5)} = 4\,\mathrm{V}^2$. Fig. 2 reads as follows. Consider for example the case $N_C = 3$, that is three colliding pulses over one-bit interval. Since $N_S = 2$ the "worst case" assumes that among the three interfering pulses, two have energy $E^{(5)}$ and one has energy $E^{(4)}$. The "best case" considers that two pulses have energy $E^{(1)}$ and one pulse has energy

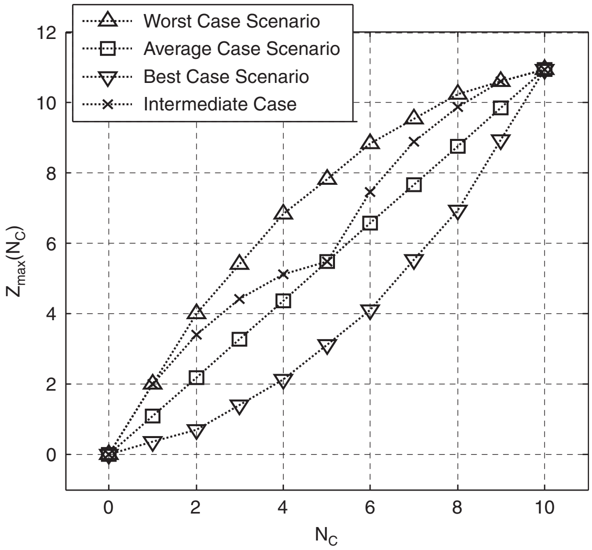

Fig. 2. Comparison of the $Z_{\max}(N_C)$ estimate with different approaches, in the special case of $N_i = 5$, $N_S = 2$, and $E^{(1)} = 1/8\,V^2$, $E^{(2)} = 1/2\,V^2$, $E^{(3)} = 1\,V^2$, $E^{(4)} = 2\,V^2$, $E^{(5)} = 4\,V^2$.

$E^{(2)}$. The "average case" considers three pulses with equivalent energy $E = (1/5\sum_{j=1}^{5}\sqrt{E^{(j)}})^2$. The "intermediate case" considers the first colliding pulse with $E^{(5)}$, the second with $E^{(4)}$, and the third with $E^{(3)}$. Fig. 2 shows that the proposed intermediate approach leads to similar MUI estimates as the worst case for the upper and lower values of N_C, i.e., for extreme MUI values (lower bound: N_C is close to zero, and upper bound: N_C is close to $N_S N_i$). Note that for N_C values close to extremes, the difference between "worst case" and "average case" estimates is minimum. For central N_C values, the difference between worst case and average estimates is maximum, while the proposed intermediate approach moves away from worst estimates to tend to average estimates.

Given $Z_{\max}(N_C)$, we can finally introduce the conditional probability function of (19) into (16). One can find the following approximate expression for the average BER at receiver output (see Appendix A for the analytical derivation):

$$\mathrm{BER} \approx Q\left(\sqrt{\frac{N_S E_u}{N_0}\gamma(\varepsilon)}\right) + \sum_{N_C=0}^{N_i N_S} \frac{P_{CP}(N_C)^2}{2}\Omega\left(\frac{N_S E_u}{N_0}\,\gamma(\varepsilon), \frac{Z_{\max}(N_C)^2}{N_S N_0 \gamma(\varepsilon)}\right), \tag{28}$$

where

$$\Omega(A,B) = Q(\sqrt{A}-\sqrt{B}) + Q(\sqrt{A}+\sqrt{B}) - 2Q(\sqrt{A}). \tag{29}$$

The BER expression in (28) includes a first term that only depends on signal to thermal noise ratio at RX input, and a second term accounting for MUI. Note that for computing (28), no additional information with respect to the BER computation with the SGA is requested.

The result in (28) provides an explicit analytical expression for the average BER at the reference receiver in the case of propagation over an AWGN channel. Note, however, that the proposed approach for modelling MUI remains valid in the presence of multipath-affected channels. When multipath propagation is taken into account, the signal at the receiver is characterized by an increased number of pulses with respect to free-space propagation. Nevertheless, interference is still provoked by collisions occurring between pulses belonging to different transmissions, and the result of (28) can be extended adjusting the number of collisions and the maximum interference term for a given number of collisions, i.e., by expanding (17) and (27) which are specific to the AWGN case. Preliminary tests of the model for a set of specific multipath-affected channel realizations indicate the validity of the adopted approach [48].

4. Simulation results

Simulation of a network of four nodes provided the results presented in Figs. 3 and 4 for two

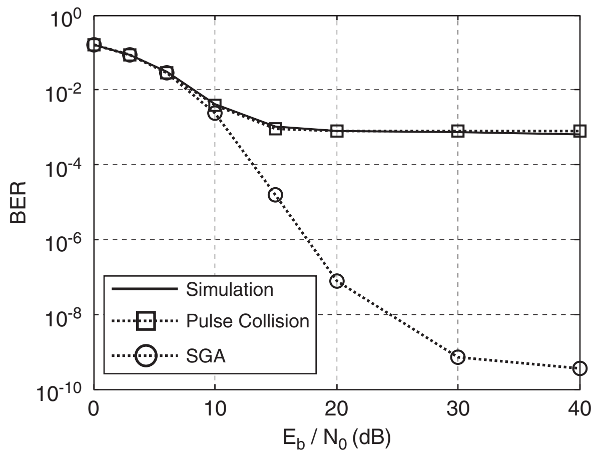

Fig. 3. BER vs. E_b/N_0 with signal format A ($N_S = 2$, $T_S = 25$ ns) and $N_i = 3$.

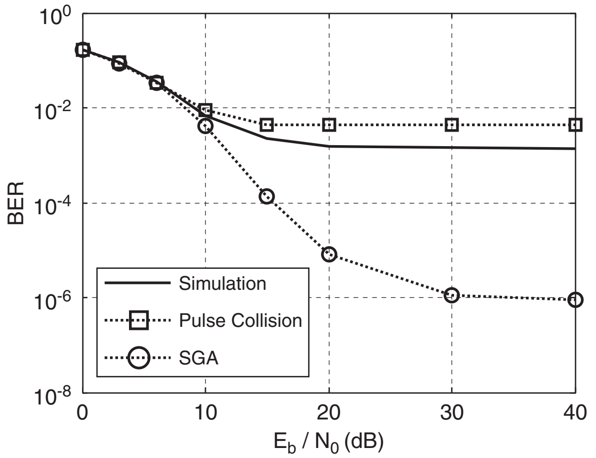

Fig. 4. BER vs. E_b/N_0 with signal format B ($N_S = 4$, $T_S = 25$ ns) and $N_i = 3$.

reference signal formats. In both cases, four users are considered ($N_i = 3$), and power control is assumed at RX. In the case of Fig. 3, transmitted signals have $N_S = 2$ and $T_S = 25$ ns, leading to $R_b = 20$ Mb/s (signal format A). In the case of Fig. 4, transmitted signals have $N_S = 4$ and $T_S = 25$ ns, leading to $R_b = 10$ Mb/s (signal format B). In both cases, $p_0(t)$ is the second derivative Gaussian waveform [33], with $T_M = 1$ ns and $\varepsilon = 1$ ns. Performance is expressed by BER vs. signal to noise ratio E_b/N_0, where $E_b = N_S E_u$ is the received energy per bit. Note that Figs. 3 and 4 are computed for same E_b, meaning that E_u is different in the two figures. Thus, one should not be surprised if performance seems to degrade from $N_S = 2$ to 4 since E_u is smaller for $N_S = 4$. In other words, the plots in Figs. 3 and 4 show that in systems affected by MUI, receiver performance does not depends only on the amount of useful energy per bit which is collected at the receiver, but it also depends on how many pulses are used for transmitting such energy. BER estimates based on Pulse Collision (squares) are plotted against simulation values (solid line) and SGA values (circles). Note that Pulse Collision values very well fit simulation data, while SGA underestimates BER.

Fig. 5 compares Pulse Collision vs. SGA for two signal formats A and B, when increasing N_i. Observe that BER estimates based on Pulse Collision are always higher than BER estimates based on SGA. The gap between the models decreases for high N_i, that is, when the number of collisions at the receiver input justifies the application of the central limit theorem. Preliminary investigations obtained

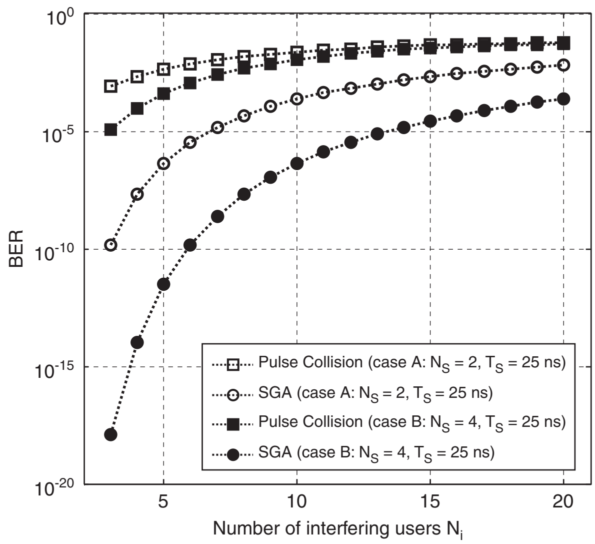

Fig. 5. Theoretical BER vs. number interfering users N_i for the two models (pulse collision and SGA) and for the two different signal formats (signal formats A and B).

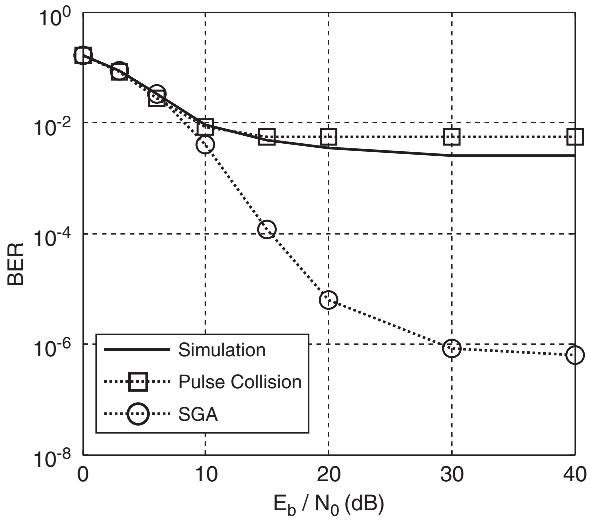

Fig. 6. BER vs. E_b/N_0 with $N_S = 1$, $T_S = 60$ ns, $N_i = 3$, $E^{(1)} = E_u$, $E^{(2)} = 4E_u$, $E^{(3)} = (1/4)E_u$.

by varying N_i and N_S seam to lead to similar network behavior.

In Figs. 6 and 7, performance of the proposed MUI model is evaluated in two different scenarios where the hypothesis of power control at RX is removed. In both cases, transmitted signals have $N_S = 1$ and $T_S = 60$ ns, leading to $R_b = 16.66$ Mb/s. In the case of Fig. 6, the network consists of one reference user with received energy per pulse E_u, and three interfering users with received energy per pulse

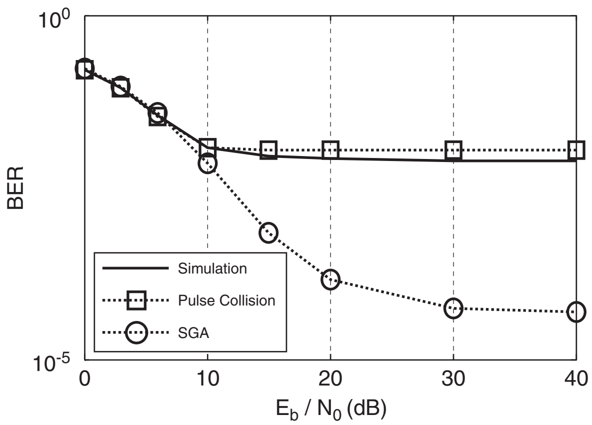

Fig. 7. BER vs. E_b/N_0 with $N_S = 1$, $T_S = 60\,\text{ns}$, $N_i = 5$, $E^{(1)} = E\text{u}$, $E^{(2)} = 4E_\text{u}$, $E^{(3)} = 8E_\text{u}$, $E^{(4)} = (1/4)\ E_\text{u}$, and $E^{(5)} = (1/8)\ E_\text{u}$.

$E^{(1)} = E_\text{u}$, $E^{(2)} = 4E_\text{u}$, and $E^{(3)} = (1/4)\ E_\text{u}$, respectively. In the case of Fig. 7, the network consists of one reference user with received energy per pulse E_u, and five interfering users with received energy per pulse $E^{(1)} = E_\text{u}$, $E^{(2)} = 4E_\text{u}$, $E^{(3)} = 8E_\text{u}$, $E^{(4)} = (1/4)\ E_\text{u}$, and $E^{(5)} = (1/8)\ E_\text{u}$, respectively. In both cases, performance is expressed by BER vs. signal to noise ratio E_u/N_0, and BER estimates based on Pulse Collision are plotted against simulation values and SGA values. By comparing the results of Figs. 6 and 7 with those of Figs. 3 and 4, one can conclude that the proposed MUI model guarantees accuracy in estimating the BER which is higher than SGA accuracy, for both power-balanced and power-unbalanced networks.

5. Conclusions

In this paper, a novel method for estimating BER in IR-UWB networks affected by MUI was presented. Differently from existing solutions, which basically extend to the UWB case results that are known for SS-CDMA systems, the proposed method analyzes MUI under a novel perspective, which explicitly takes into account the peculiar way in which information is structured and conveyed by IR-UWB devices. In IR-UWB, information bits are coded into sequences of short pulses. MUI can thus be re-analyzed by observing that interference at the reference receiver is provoked by collisions occurring between pulses belonging to different transmissions. Based on this observation, a novel analytical expression for the average BER was derived for the reference scenario where IR-UWB-PPM-TH signals propagate over AWGN channels, and terminals adopt single user receivers with soft decision detection.

The proposed approach showed high accuracy in estimating receiver performance by simulation of different network topologies. Results were presented for both power-controlled and power-unbalanced systems. Estimation accuracy provided by the proposed method results to be much higher than that provided by conventional Gaussian-based approaches, in particular when scarcely populated systems, or systems with dominating interferers, or low-rate systems are taken into account. Differently from existing non-Gaussian approaches, however, the proposed approach does neither require knowledge of additional system parameters, as in GQR methods, nor necessitates numerical computation of open-ended integrals, as in the CF method. Note that the adopted Pulse Collision approach is applicable in a straightforward manner to other IR signal formats, such as PAM-TH-UWB or DS-UWB.

A natural extension of this work is to include propagation over multipath-affected channels. The Pulse Collision approach presented in this paper is in fact flexible enough to include improved sophistications of receiver structures, such as RAKE, and as such promises to be effective for predicting the behavior of complex UWB networks.

Appendix A. Analytical derivation of the average BER in the Pulse Collision model

In this appendix, we illustrate the derivation of the average BER at the receiver output following the Pulse Collision approach. According to Section 3, the average BER can be evaluated by introducing the conditional probability function of (19) into (16). One has

$$
\begin{aligned}
\text{BER} = \sum_{N_\text{C}=0}^{N_\text{S}N_\text{i}} P_\text{CP}(N_\text{C}) \Bigg[& \int_{-\infty}^{-Z_{\max}(N_\text{C})} p_Y(y)\,\mathrm{d}y \\
& + \int_{-Z_{\max}(N_\text{C})}^{0} p_Y(y)\,\mathrm{d}y \\
& - \frac{P_\text{CP}(N_\text{C})}{2} \int_{-Z_{\max}(N_\text{C})}^{0} p_Y(y)\,\mathrm{d}y \\
& - \frac{P_\text{CP}(N_\text{C})}{2Z_{\max}(N_\text{C})} \int_{-Z_{\max}(N_\text{C})}^{0} y p_Y(y)\,\mathrm{d}y
\end{aligned}
$$

$$
\begin{aligned}
&+\frac{P_{\mathrm{CP}}(N_{\mathrm{C}})}{2}\int_{0}^{+Z_{\max}(N_{\mathrm{C}})} p_Y(y)\,\mathrm{d}y \\
&-\frac{P_{\mathrm{CP}}(N_{\mathrm{C}})}{2Z_{\max}(N_{\mathrm{C}})}\int_{0}^{+Z_{\max}(N_{\mathrm{C}})} y p_Y(y)\,\mathrm{d}y\Bigg] \\
&=\left(\sum_{N_{\mathrm{C}}=0}^{N_{\mathrm{S}}N_{\mathrm{i}}} P_{\mathrm{CP}}(N_{\mathrm{C}})\right)\int_{-\infty}^{0} p_Y(y)\,\mathrm{d}y \\
&+\sum_{N_{\mathrm{C}}=0}^{N_{\mathrm{S}}N_{\mathrm{i}}}\frac{P_{\mathrm{CP}}(N_{\mathrm{C}})^2}{2}\left[-\int_{-Z_{\max}(N_{\mathrm{C}})}^{0} p_Y(y)\,\mathrm{d}y\right. \\
&+\int_{0}^{+Z_{\max}(N_{\mathrm{C}})} p_Y(y)\,\mathrm{d}y \\
&\left.-\frac{1}{Z_{\max}(N_{\mathrm{C}})}\int_{-Z_{\max}(N_{\mathrm{C}})}^{+Z_{\max}(N_{\mathrm{C}})} y p_Y(y)\,\mathrm{d}y\right] \\
&=\int_{-\infty}^{0} p_Y(y)\,\mathrm{d}y+\sum_{N_{\mathrm{C}}=0}^{N_{\mathrm{S}}N_{\mathrm{i}}}\frac{P_{\mathrm{CP}}(N_{\mathrm{C}})^2}{2} \\
&\times\left[-\int_{-\infty}^{0} p_Y(y)\,\mathrm{d}y+\int_{-\infty}^{-Z_{\max}(N_{\mathrm{C}})} p_Y(y)\,\mathrm{d}y\right. \\
&+\int_{-\infty}^{+Z_{\max}(N_{\mathrm{C}})} p_Y(y)\,\mathrm{d}y-\int_{-\infty}^{0} p_Y(y)\,\mathrm{d}y \\
&\left.-\frac{1}{Z_{\max}(N_{\mathrm{C}})}\int_{-Z_{\max}(N_{\mathrm{C}})}^{+Z_{\max}(N_{\mathrm{C}})} y p_Y(y)\,\mathrm{d}y\right] \\
&=\int_{-\infty}^{0} p_Y(y)\,\mathrm{d}y+\sum_{N_{\mathrm{C}}=0}^{N_{\mathrm{S}}N_{\mathrm{i}}}\frac{P_{\mathrm{CP}}(N_{\mathrm{C}})^2}{2} \\
&\times\left[\int_{-\infty}^{-Z_{\max}(N_{\mathrm{C}})} p_Y(y)\,\mathrm{d}y\right. \\
&+\int_{-\infty}^{+Z_{\max}(N_{\mathrm{C}})} p_Y(y)\,\mathrm{d}y-2\int_{-\infty}^{0} p_Y(y)\,\mathrm{d}y \\
&\left.-\frac{1}{Z_{\max}(N_{\mathrm{C}})}\int_{-Z_{\max}(N_{\mathrm{C}})}^{+Z_{\max}(N_{\mathrm{C}})} y p_Y(y)\,\mathrm{d}y\right], \qquad (30)
\end{aligned}
$$

where $p_Y(y)$ is the probability density function of the Gaussian random variable y, which has mean value $y_{\mathrm{m}} = N_{\mathrm{S}}\sqrt{E_{\mathrm{u}}}\gamma(\varepsilon)$ and variance ${\sigma_y}^2 = N_{\mathrm{S}}N_0\gamma(\varepsilon)$, i.e.

$$
p_Y(y)=\frac{1}{\sqrt{2\pi N_{\mathrm{S}}N_0\gamma(\varepsilon)}}\,\mathrm{e}^{-(y-N_S\sqrt{E_u}\gamma(\varepsilon))^2/2N_SN_0\gamma(\varepsilon)}. \qquad (31)
$$

By introducing the function $Q(x)$, defined as

$$
Q(x)=(2\pi)^{-1/2}\int_{x}^{\infty}\mathrm{e}^{-t^2/2}\,\mathrm{d}t \qquad (32)
$$

and by applying the property

$$
1-Q(-x)=Q(x). \qquad (33)
$$

Eq. (30) rewrites

$$
\begin{aligned}
\mathrm{BER}&=Q\left(\frac{N_{\mathrm{S}}\sqrt{E_{\mathrm{u}}}\gamma(\varepsilon)}{\sqrt{N_{\mathrm{S}}N_0\gamma(\varepsilon)}}\right) \\
&+\sum_{N_{\mathrm{C}}=0}^{N_{\mathrm{S}}N_{\mathrm{i}}}\frac{P_{\mathrm{CP}}(N_{\mathrm{C}})^2}{2}\left[-2Q\left(\frac{N_{\mathrm{S}}\sqrt{E_{\mathrm{u}}}\gamma(\varepsilon)}{\sqrt{N_{\mathrm{S}}N_0\gamma(\varepsilon)}}\right)\right. \\
&+Q\left(\frac{N_{\mathrm{S}}\sqrt{E_{\mathrm{u}}}\gamma(\varepsilon)-Z_{\max}(N_{\mathrm{C}})}{\sqrt{N_{\mathrm{S}}N_0\gamma(\varepsilon)}}\right) \\
&+Q\left(\frac{N_{\mathrm{S}}\sqrt{E_{\mathrm{u}}}\gamma(\varepsilon)+Z_{\max}(N_{\mathrm{C}})}{\sqrt{N_{\mathrm{S}}N_0\gamma(\varepsilon)}}\right) \\
&\left.-\frac{1}{Z_{\max}(N_{\mathrm{C}})}\int_{-Z_{\max}(N_{\mathrm{C}})}^{+Z_{\max}(N_{\mathrm{C}})} y p_Y(y)\,\mathrm{d}y\right] \\
&=Q\left(\sqrt{\frac{N_{\mathrm{S}}E_{\mathrm{u}}}{N_0}}\gamma(\varepsilon)\right) \\
&+\sum_{N_{\mathrm{C}}=0}^{N_{\mathrm{S}}N_{\mathrm{i}}}\frac{P_{\mathrm{CP}}(N_{\mathrm{C}})^2}{2}\left[-2Q\left(\sqrt{\frac{N_{\mathrm{S}}E_{\mathrm{u}}}{N_0}}\gamma(\varepsilon)\right)\right. \\
&+Q\left(\sqrt{\frac{N_{\mathrm{S}}E_{\mathrm{u}}}{N_0}}\gamma(\varepsilon)-\sqrt{\frac{Z_{\max}(N_{\mathrm{C}})^2}{N_{\mathrm{S}}N_0\gamma(\varepsilon)}}\right) \\
&+Q\left(\sqrt{\frac{N_{\mathrm{S}}E_{\mathrm{u}}}{N_0}}\gamma(\varepsilon)+\sqrt{\frac{Z_{\max}(N_{\mathrm{C}})^2}{N_{\mathrm{S}}N_0\gamma(\varepsilon)}}\right) \\
&\left.-\frac{1}{Z_{\max}(N_{\mathrm{C}})}\int_{-Z_{\max}(N_{\mathrm{C}})}^{+Z_{\max}(N_{\mathrm{C}})} y p_Y(y)\,\mathrm{d}y\right]. \qquad (34)
\end{aligned}
$$

Since $p_Y(y)$ is always positive and symmetrical around its mean value $y_{\mathrm{m}} > 0$, it is easy to recognize that the last term in (34) is always negative. One thus obtains

$$
\begin{aligned}
&\mathrm{BER}\leqslant\mathrm{BER}_{\mathrm{upbound}} \\
&=Q\left(\sqrt{\frac{N_{\mathrm{S}}E_{\mathrm{u}}}{N_0}}\gamma(\varepsilon)\right) \\
&+\sum_{N_{\mathrm{C}}=0}^{N_{\mathrm{S}}N_{\mathrm{i}}}\frac{P_{\mathrm{CP}}(N_{\mathrm{C}})^2}{2}\left[-2Q\left(\sqrt{\frac{N_{\mathrm{S}}E_{\mathrm{u}}}{N_0}}\gamma(\varepsilon)\right)\right. \\
&+Q\left(\sqrt{\frac{N_{\mathrm{S}}E_{\mathrm{u}}}{N_0}}\gamma(\varepsilon)-\sqrt{\frac{Z_{\max}(N_{\mathrm{C}})^2}{N_{\mathrm{S}}N_0\gamma(\varepsilon)}}\right) \\
&\left.+Q\left(\sqrt{\frac{N_{\mathrm{S}}E_{\mathrm{u}}}{N_0}}\gamma(\varepsilon)+\sqrt{\frac{Z_{\max}(N_{\mathrm{C}})^2}{N_{\mathrm{S}}N_0\gamma(\varepsilon)}}\right)\right], \qquad (35)
\end{aligned}
$$

If we approximate the BER with its upper bound given in (35), we have

$$\mathrm{BER} \approx Q(\sqrt{A}) + \sum_{N_C=0}^{N_S N_i} \frac{P_{CP}(N_C)^2}{2} (Q(\sqrt{A} - \sqrt{B}) + Q(\sqrt{A} + \sqrt{B}) - 2Q(\sqrt{A})), \quad (36)$$

where we have substituted

$$A = \frac{N_S E_u}{N_0} \gamma(\varepsilon), \quad B = \frac{Z_{max}(N_C)^2}{N_S N_0 \gamma(\varepsilon)} \quad (37)$$

which leads to the BER expression in (28).

References

[1] M.-G. Di Benedetto, G. Giancola, Understanding Ultra Wide Band Radio Fundamentals, Prentice-Hall, Upper Saddle River, NJ, 2004.

[2] M. Pursley, Performance evaluation for phase-coded spread-spectrum multiple-access communication—Part I: system analysis, IEEE Trans. Commun. 25 (8) (1977) 795–799.

[3] Y. Asano, Y. Daido, J.M. Holtzman, Performance evaluation for band-limited DS-CDMA communication system, in: Proceedings of the IEEE Vehicular Technology Conference 1993 (VTC 1993), pp. 464–468.

[4] G.P. Efthymoglou, V.A. Aalo, H. Helmken, Performance analysis of coherent DS-CDMA systems in a Nakagami fading channel with arbitrary parameters, IEEE Trans. Veh. Technol. 46 (2) (1997) 289–297.

[5] K.S. Gilhousen, I.M. Jacobs, R. Padovani, A.J. Viterbi, L.A. Weaver Jr., C.E. Wheatley III, On the capacity of a cellular CDMA system, IEEE Trans. Veh. Technol. 40 (2) (1991) 303–312.

[6] Zhao Liu, M. El Zarki, SIR-based call admission control for DS-CDMA cellular systems, IEEE J. Sel. Areas Commun. 12 (4) (1994) 638–644.

[7] Wen-Bin Yang, E. Geraniotis, Admission policies for integrated voice and data traffic in CDMA packet radio networks, IEEE J. Sel. Areas Commun. 12 (4) (1994) 654–664.

[8] Seung Joon Lee, Hyeon Woo Lee, Dan Keun Sung, Capacities of single-code and multicode DS-CDMA systems accommodating multiclass services, IEEE Trans. Veh. Technol. 48 (2) (1999) 376–384.

[9] T.H. Hu, M.M.K. Liu, A new power control function for multirate DS-CDMA systems, IEEE Trans. Commun. 47 (6) (1999) 896–904.

[10] M.O. Sunay, P.J. McLane, Calculating error probabilities for DS CDMA systems: When not to use the Gaussian approximation, in: Proceedings of the IEEE Global Communication Conference 1996 (GLOBECOM 1996), pp. 1744–1749.

[11] Y.C. Yoon, A simple and accurate method of probability of bit error analysis for asynchronous band-limited DS-CDMA systems, IEEE Trans. Commun. 50 (4) (2002) 656–663.

[12] R.K. Morrow, J.S. Lehnert, Bit-to-bit error dependence in slotted DS/SSMA packet systems with random signature sequences, IEEE Trans. Commun. 37 (10) (1989) 1052–1061.

[13] R.K. Morrow, J.S. Lehnert, Packet throughput in slotted ALOHA DS/SSMA radio systems with random signature sequences, IEEE Trans. Commun. 40 (1992) 1223–1230.

[14] J.C. Liberti, T.S. Rappaport, Accurate techniques to evaluate CDMA bit error rates in multipath channels with imperfect power control, in: Proceedings of the IEEE Global Telecommunications Conference (GLOBECOM 1995), 1995, pp. 33–37.

[15] J.M. Holtzman, A simple, accurate method to calculate spread-spectrum multiple-access error probabilities, IEEE Trans. Commun. 40 (3) (1992) 461–464.

[16] R.K. Morrow Jr., Accurate CDMA BER calculations with low computational complexity, IEEE Trans. Commun. 46 (11) (1998) 1413–1417.

[17] H.H. Nguyen, E. Shwedyk, On error probabilities of DS-CDMA systems with arbitrary chip waveforms, IEEE Commun. Lett. 5 (3) (2001) 78–80.

[18] J.M. Holtzman, On using perturbation analysis to do sensitivity analysis: derivatives vs. differences, in: Proceedings of the 28th IEEE Conference on Decision and Control, 1989, pp. 2018–2023.

[19] K.B. Letaief, J.C. Chuang, J.S. Sadowsky, BER estimation of asynchronous DS/CDMA communications systems, in: Proceedings of the IEEE International Conference on Communications, 1995 (ICC 95), vol. 3, pp. 1340–1344.

[20] E. Geraniotis, M. Pursley, Error probability for direct-sequence spread-spectrum multiple-access communications—Part II: approximations, IEEE Trans. Commun. 30 (5) (1982) 985–995.

[21] E. Geraniotis, B. Ghaffari, Performance of binary and quaternary direct-sequence spread-spectrum multiple-access systems with random signature sequences, IEEE Trans. Commun. 39 (5) (1991) 713–724.

[22] G.E. Corazza, G. De Maio, F. Vatalaro, CDMA cellular systems performance with fading, shadowing, and imperfect power control, IEEE Trans. Veh. Technol. 47 (2) (1998) 450–459.

[23] O. Shimbo, M. Celebiler, The probability of error due to intersymbol interference and Gaussian Noise in digital communication systems, IEEE Trans. Commun. 19 (2) (1971) 113–119.

[24] J. Vanelli, N. Shehadeh, Computation of bit-error probability using the trapezoidal integration rule, IEEE Trans. Commun. 22 (3), 331–334.

[25] K.E. Atkinson, An Introduction to Numerical Analysis, second ed, Wiley, New York, 1989.

[26] D. Laforgia, A. Luvison, V. Zingarelli, Bit error rate evaluation for spread-spectrum multiple-access systems, IEEE Trans. Commun. 32 (6) (1984) 660–669.

[27] G.H. Golub, J.H. Welch, Calculation of Gaussian quadrature rules, in: Mathematics of Computation, American Mathematical Society, vol. 23, 1969, pp. 221–230.

[28] R. Dogliotti, A. Luvison, G. Pirani, Error probability in optical fiber transmission systems, IEEE Trans. Inform. Theory 25 (1979) 170–178.

[29] S. Benedetto, G. De Vincentis, A. Luvison, Error probability in the presence of intersymbol interference and additive noise for multilevel digital signals, IEEE Trans. Commun. 21 (1973) 181–190.

[30] W.H. Lam, R. Steele, Performance of direct-sequence spread-spectrum multiple-access systems in mobile radio, IEE Proc. Commun. Speech Vision 138 (1) (1991) 1–14.

[31] K.-T. Wu, S.-A. Tsaur, Error performance for diversity DS-SSMA communications in fading channels, IEE Proc. 141 (5) (1994) 357–363.
[32] R. Scholtz, Multiple access with time-hopping impulse modulation, in: Proceedings of the IEEE Military Communications Conference 1993 (MILCOM '93), vol. 2, pp. 447–450.
[33] M.Z. Win, R.A. Scholtz, Ultra-wide bandwidth time-hopping spread-spectrum impulse radio for wireless multiple access communications, IEEE Transactions on Communications 48 (4) (2000) 679–689.
[34] F. Cuomo, C. Martello, A. Baiocchi, F. Capriotti, Radio resource sharing for ad hoc networking with UWB, IEEE J. Sel. Areas Commun. 20 (9) (2002) 1722–1732 (special issue on Ultra Wide Band Radio in Multi-Access Wireless Networks).
[35] I. Güvenc, H. Arslan, S. Gezici, H. Kobayashi, Adaptation of multiple access parameters in time hopping UWB cluster based wireless sensor networks, in: Proceedings of the IEEE International Conference on Mobile Ad-hoc and Sensor Systems 2004 (MASS 2004).
[36] B. Radunovic, J.-Y. Le Boudec, Optimal power control, scheduling, and routing in UWB networks, IEEE J. Sel. Areas Commun. 22 (7) (2004) 1252–1270.
[37] G. Giancola, C. Martello, F. Cuomo, M.-G. Di Benedetto, Radio resource management in infrastructure-based and ad hoc UWB networks, Wireless Commun. Mobile Comput. J. (2005) (special issue on Ultra Wideband Communications).
[38] G. Durisi, G. Romano, On the validity of Gaussian approximation to characterize the multiuser capacity of UWB TH PPM, in: Proceedings of the IEEE Conference on Ultra Wideband Systems and Technologies 2002, (UWBST 2002), pp. 157–161.
[39] G. Giancola, L. De Nardis, M.-G. Di Benedetto, Multi user interference in power-unbalanced ultra wide band systems: analysis and verification, in: Proceedings of the IEEE Conference on Ultra Wideband Systems and Technologies 2003 (UWBST 2003), pp. 325–329.
[40] J. Fiorina, W. Hachem, Central limit results for the multiple user interference at the SUMF output for UWB signals, in: Proceedings of the International Symposium on Information Theory and its Applications 2004 (ISITA 2004).
[41] W. Feller, An Introduction to Probability Theory and Its Applications, third ed, Wiley, New York, 1968.
[42] Hu Bo, N.C. Beaulieu, Accurate evaluation of multiple-access performance in TH-PPM and TH-BPSK UWB systems, IEEE Trans. Commun. 52 (10) (2004) 1758–1766.
[43] A.R. Forouzan, M. Nasiri-Kenari, J.A. Salehi, Performance analysis of time-hopping spread-spectrum multiple-access systems: uncoded and coded schemes, IEEE Trans. Wireless Commun. 1 (4) (2002) 671–681.
[44] M. Sabattini, E. Masry, L.B. Milstein, A non-Gaussian approach to the performance analysis of UWB TH-BPPM systems, in: Proceedings of the IEEE Conference on Ultra Wideband Systems and Technologies 2003 (UWBST 2003), pp. 52–55.
[45] G. Durisi, S. Benedetto, Performance evaluation of TH-PPM UWB systems in the presence of multiuser interference, IEEE Commun. Lett. 7 (5) (2003) 224–226.
[46] J.R. Fontana, An insight into UWB interference from a shot noise perspective, in: Proceedings of the IEEE Conference on Ultra Wide Band Systems and Technologies 2002 (UWBST 2002), pp. 309–313.
[47] M.-G. Di Benedetto, L. De Nardis, M. Junk, G. Giancola, (UWB)ˆ2: Uncoordinated, Wireless, Baseborn, medium access control for UWB communication networks, Mobile Networks Appl. J. (2005) (special issue on WLAN Optimization at the MAC and Network Levels).
[48] L. De Nardis, G. Giancola, M.-G. Di Benedetto, Robustness of uncoordinated MAC in channel impaired low data rate UWB networks, INFOCOM Department Internal Report, Sector 4, 2005, No. 001.